Journal of the European Ceramic Society **11** (1993) 231–236

The Synthesis of SiC–B_4C Ceramics by Combustion during Hot-Pressing

Z. Pánek

Institute of Inorganic Chemistry, Slovak Academy of Sciences, Dúbravská cesta 9, CS-842 36 Bratislava, Czech Republic

(Received 22 April 1992; accepted 2 June 1992)

Abstract

Using powders of Si, B and carbon black as reactants a material having a very low porosity (<1%) and uniform microstructure was synthesized by the combustion hot-pressing method. The composition of the material corresponds to the equal volumes of SiC and B_4C. The microstructure consists of two interlocked matrices formed by carbides and pores. No residues of starting reagents were observed in the products.

Ausgehend von Si-, B- und C-Pulvern als Reaktanten wurde ein Material mit sehr geringer Porosität (weniger als 1%) und mit gleichmäßigem Gefüge mittels reaktivem Heißpressen synthetisiert. Das Material besteht zu gleichen Volumenanteilen aus SiC und B_4C. Sein Gefüge baut sich aus zwei zusammenhängenden Matrizes aus den Karbiden und Poren auf. Im Produktmaterial können keine Restbestände der Ausgangsreaktanten festgestellt werden.

L'utilisation de poudres de Si, B et noir de carbone en tant que réactifs dans la méthode de combustion par compression uniaxiale à chaud, a permis la synthèse d'un matériau présentant une porosité très faible (<1%) et une microstructure uniforme. La composition du matériau correspond à un volume équivalent de SiC et de B_4C. La microstructure consiste en deux matrices imbriquées formées par les carbures et des pores. On ne relève aucun résidu des matières premières dans les produits de la réaction.

1 Introduction

Most advanced ceramics are manufactured by the conventional processing route. However, this method, based on the nearly identical phase composition of starting powder and final product, seems to be rather disadvantageous, particularly for 'pure' systems, because the excess of surface Gibbs' energy is the only driving force for the densification process. The excess of surface energy is often insufficient for the required densification. Therefore, sintering aids or external pressure are commonly used to accelerate mass transport during sintering. However, sintering aids cause a deterioration in the mechanical properties of the material, particularly at high temperatures. Because advanced ceramics are synthetic materials, a major effort is devoted to the problem of direct synthesis of ceramics in nearly net shape form. Despite the fact that this goal is expected to be achieved by the thermal decomposition of organometallic compounds,[1–4] other methods, such as self-propagating high-temperature synthesis (SHS),[5] sol–gel and reaction bonding, may also lead to the direct synthesis of high-quality materials.

The aim of this work was to estimate the possibility of combining the SHS technique and hot-pressing (HP) into an acceptable method (called here combustion hot-pressing, CHP) for the synthesis of ceramics. Particularly for systems which have constant mass of solid during chemical reactions and higher densities of final products than the starting reagents, the proposed method may be advantageous, because the volume contraction during combustion may be simultaneously eliminated by the external force. The Si (density $d = 2{\cdot}33\ \mathrm{g\ cm^{-3}}$)–B ($d = 2{\cdot}34\ \mathrm{g\ cm^{-3}}$)–C ($d = 2{\cdot}26\ \mathrm{g\ cm^{-3}}$) starting system was chosen and SiC–B_4C material, being characterized by two interlocked matrices and a low porosity, has been expected as the final shaped product.

2 Experimental

The starting reagents used in this study were semiconductor silicon platelets (Tesla, ČSFR), boron powder from Schuchardt (FRG; amorphous, maximum particle size 1·5 μm, 95–97 mass% B, Mg <1·2%, Fe <0·2%, Si <0·2%, O <4%, N <1·5%),

Journal of the European Ceramic Society 0955-2219/93/$6.00

high purity acetylene carbon black ($S_{BET} = 80\,m^2\,g^{-1}$) from Stickstoffwerk Piesteritz (FRG), and SiC (98·8%, main impurities Fe, Ti, Ni, Al, V) and B_4C (B/C = 4·1) powders from Ventron Alfa (FRG).

The silicon platelets were, after grinding and wet ball-milling (isopropanol), dried, purified (HCl), separated by sedimentation and subsequently analysed (99·9% Si, maximum grain size 5 μm). Two mixtures, Si–B–C (SBC) and SiC–B_4C (SB), were prepared from the powder by attrition milling and homogenization in isopropanol for 4 h using SiC milling media. The dried and disintegrated mixtures were used for this study. The maximum grain sizes observed in the optical microscope were about 3 and 5 μm for the SBC and SB mixtures, respectively. The chemical composition of all mixtures correspond to the equal volume of SiC and B_4C. The impurity content in B as well as the solubility of B in SiC (8%)[6] were taken into account in the calculation of SBC composition.

DTA and dilatometric studies (mass of samples about 0·15 g) were undertaken so that the temperature range and heating rate necessary for the SHS initiation as well as volume change could be observed.

The consolidation of powder mixtures was performed in a laboratory hot press[7] at a pressure of 0·1–30 MPa and heating rate of 15–150°C min^{-1} up to 1900°C in dry argon atmosphere. The dwell at the maximum temperature was 30 min, 60 min or until zero shrinkage rate occurred. Six different temperature—pressure schedules (a–f in Fig. 1) were selected for the consolidation process. About 0·3 g of the powder mixture was pressed in a 7 mm inside diameter graphite die. The sample was separated from the graphite die walls by a thin (0·05 mm) boron nitride layer.

Final densities were measured in mercury according to Archimedes' principle and their values are summarized, together with the corresponding processing data, in Table 1. The approximate density

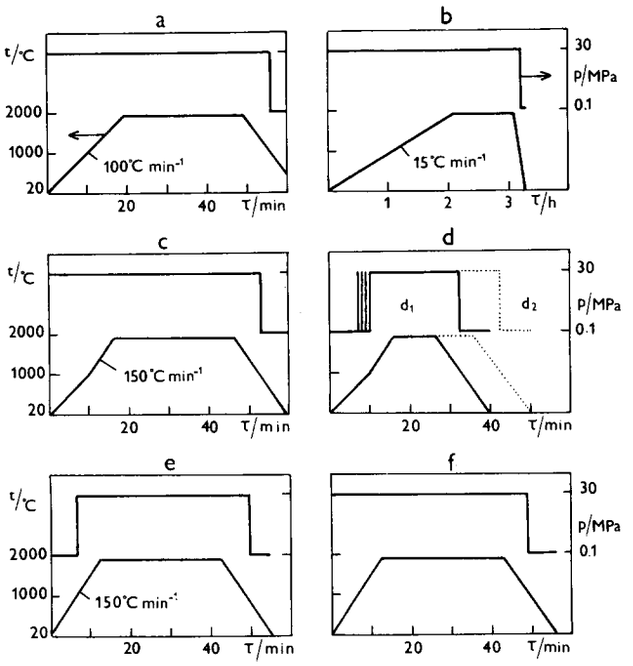

Fig. 1. Temperature–pressure treatment schedule; cooling rate 150°C min^{-1} for all experiments.

of an equivolume mixture of SB (2·863 g cm^{-3}) was calculated from SiC (3·217 g cm^{-3}) and B_4C (2·51 g cm^{-3}) densities, neglecting their mutual solubility. The calculated density of a poreless mixture, SBC, is 2·316 g cm^{-3}. Hence, the difference between the densities of SBC and SB mixtures causes the predicted volume contraction of 19·1% when the SBC mixture is converted to the SB one.

XRD analysis was undertaken to identify the crystal phases present after different stages of heat or HP treatment. The microstructures of sintered materials were studied on fracture surfaces and polished sections by SEM and optical microscopy.

3 Results and Discussion

DTA analysis data of SBC mixtures (Fig. 2) show the character of exotherms at the different heating rates.

Table 1. Characteristics of treatments and products

Experiment sample number	*Mixture*	*Treatment schedule[a]/dwell at 1900°C (min)*	*Density[b] (g cm^{-3})*	*Porosity (%)*	*SR ($mm\,h^{-1}$)*	*FSR ($mm\,h^{-1}$)*
I	SiC–B_4C	a/30	2·50	12·7	4·33	0·26
II	Si–B–C	b/60	2·75	3·9	5·40	0·33
III	Si–B–C	a/30	2·74	4·3	32·14	0·14
IV	Si–B–C	c/30	2·77	3·2	56·25	0·07
V	Si–B–C	d_1/10	2·84	0·9	48·91	$<10^{-2}$
VI	Si–B–C	d_2/20	2·85	0·3	50·10	$<10^{-3}$
VII	Si–B–C	f/30	2·62	8·5	28·12	0·20
VIII	Si–B–C	e/30	2·68	6·4	37·50	0·29

[a] See Fig. 1.
[b] $\sigma = 0{\cdot}0085$ g cm^{-3}.
SR, Linear shrinkage rate at 1800°C. FSR, Linear shrinkage rate at the end of the experiment.

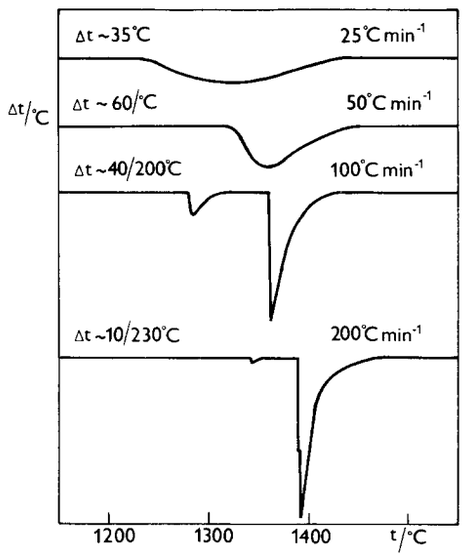

Fig. 2. DTA curves for Si–B–C powder mixtures at different heating rate; Δt is the maximum temperature difference for first and second exotherm, respectively.

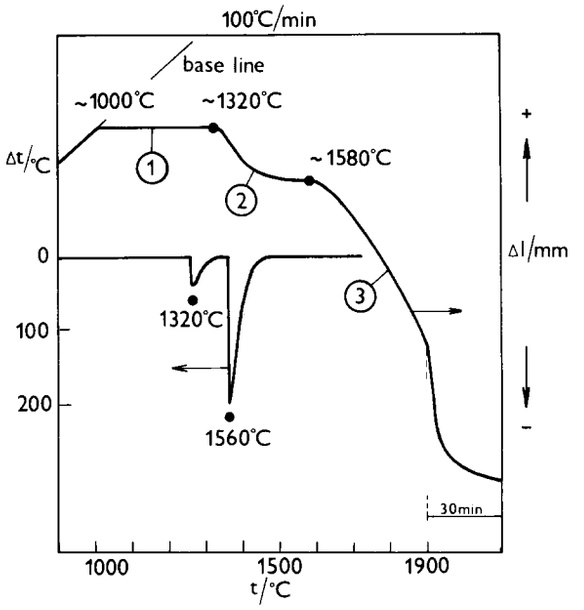

Fig. 3. Dilatometric curve of CHP and corresponding DTA curve for sample labelled as III in Table 1. 1, Non-combustion; 2, combustion; 3, post-combustion stage of densification. Baseline represents the HP dilatometric curve of system die pistons–graphite sample.

As can be seen, a minimum heating rate between 50 and 100°C min^{-1} is necessary to initiate the combustion synthesis. At a lower heating rate (non-combustion synthesis) only one broad exotherm was observed. This behaviour agrees with the thermodynamic analysis for simultaneous reactions according to the equation

$$Si + 4B + C \rightarrow xSiC + yB_4C + aSi + bB + (cC \rightarrow 0)$$

Formation of silicides was omitted for the lack of thermochemical data. The calculated[8] x/y ratios are 1 and 0·8 at 1300 and 2100 K, respectively. The XRD analysis confirms the simultaneous formation of SiC and B_4C at temperatures between 1100–1700°C. The dilatometric curve corresponding to the non-combustion HP is shown in Fig. 4(II). No sharp changes in dilatometric curve, lower linear shrinkage rate (SR) and higher linear shrinkage rate at the end of the experiment (FSR) compared to CHP were observed (see Table 1).

Depending on the heating rate, thermocouple location in the sample, and particle size and packing, one to three sharp asymmetric exothermic peaks (most frequently two peaks) were observed by DTA (Fig. 2) at heating rates $\geq$100°C min^{-1}. The exotherms were observed in the temperature range between 1260 and 1390°C, and they shifted to higher temperatures and were closer together at heating rates >100°C min^{-1}. The mean temperature increase rate during combustion was 100°C s^{-1}. Because the thermal expansions of sample and die pistons could not be determined during the combustion and post-combustion periods, an unconventional depiction of dilatometric curves was used in Figs 3 and 4. As can be seen in Fig. 3 (see also Fig. 4(III–V)), there are three stages of densification during CHP. The first stage is characterized by reactions without combustion (1000–1300°C), the second one is a combustion (1300–1400°C) and the third stage is conventional HP (1400–1900°C). An explanation of exothermic effects by XRD has been unsuccessful because the cooling rate of samples at both DTA and HP methods was insufficient.

The impurities in boron promote the formation of silicides[9] and carbides, so that relatively low initial shrinkage temperatures about 1000°C at HP of SBC mixture were observed (Figs 3 and 4). Because formation of all the solid products is accompanied by a volume contraction in the range of 5·5% for B_6Si to 28·2% for SiC and the reaction system is under pressure, shrinkage occurs as soon as the reactions start. As expected, the maximum shrinkage rate (700 mm min^{-1}) was determined during the second combustion period. No starting reagents were detected by XRD and optical microscopy after this period.

Figure 4 shows typical dilatometric curves for HP and CHP densification with substantial differences among them. The different densification kinetics during pressureless or HP consolidation as well as final properties of SiC–B_4C materials have been described and discussed elsewhere.[6,11,12] Further discussion will concern the CHP process.

In agreement with the results of Ref. 13, the volume increase in the temperature range 900–1500°C and high temperature (>1900°C) necessary for pressureless densification controlled by diffusion mechanisms was observed by dilatometric methods at the heating rate 15–100°C min^{-1} for SBC samples, as a consequence of directional formation of columnar B_4C in graphite. On the other hand, no

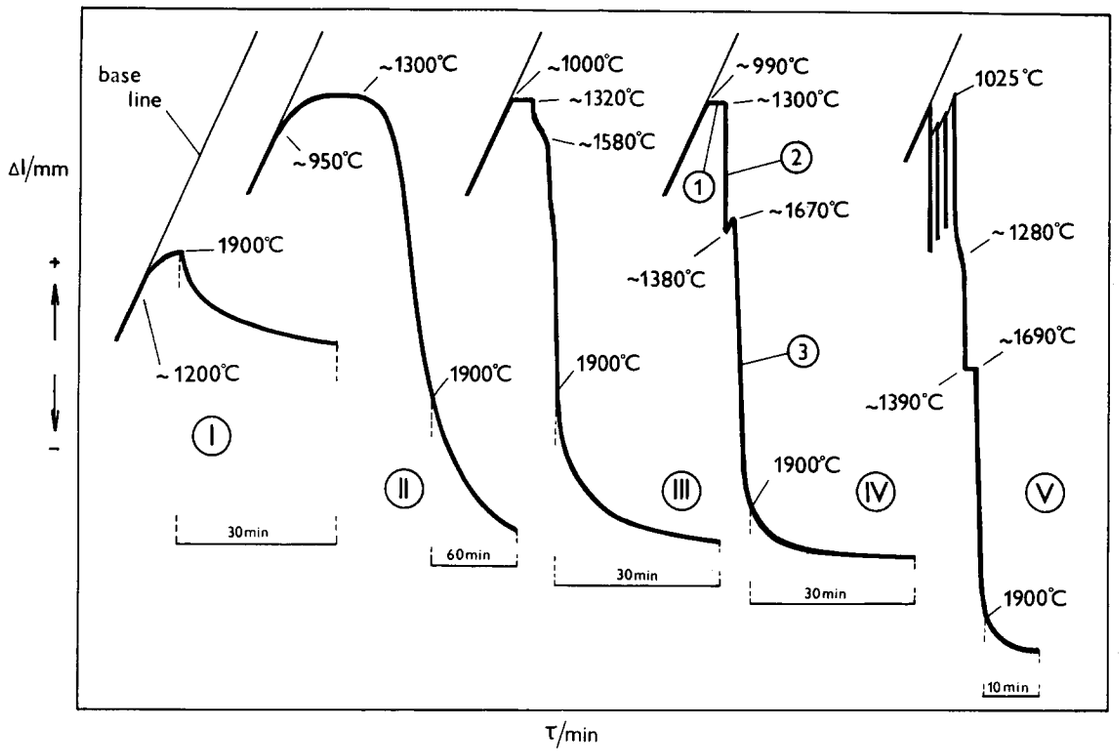

Fig. 4. Dilatometric curves of HP (I and II) and CHP (III–V) densification methods. Samples are labelled in accordance with Table 1.

volume increase and considerably lower temperatures necessary for densification (1000°C) were observed during HP or CHP. However, it is assumed that B_4C formation in the described form also exists during HP before the ignition of reactive mixture. The formation of carbides before ignition lowers the temperature during combustion and the columnar form of B_4C makes the reaction system more rigid. Hence, it may be expected that the densification during the combustion period decreases as the carbide content formed before ignition increases. Consequently, more diffusional mass transport is needed to eliminate the porosity in the final stage of densification. This explanation is supported by the results of all the experiments. It is assumed that at a higher heating rate a smaller amount of carbides is formed before the ignition. Then the combustion process starts with a higher reaction activity of mixture, resulting in a greater densification contribution during the combustion.

The highest final densities of samples were achieved using the treatment schedules d_1 and d_2 (Table 1; Figs 1, 8, 10 and 11), which are characterized by the discontinuous pressure in the initial stage of

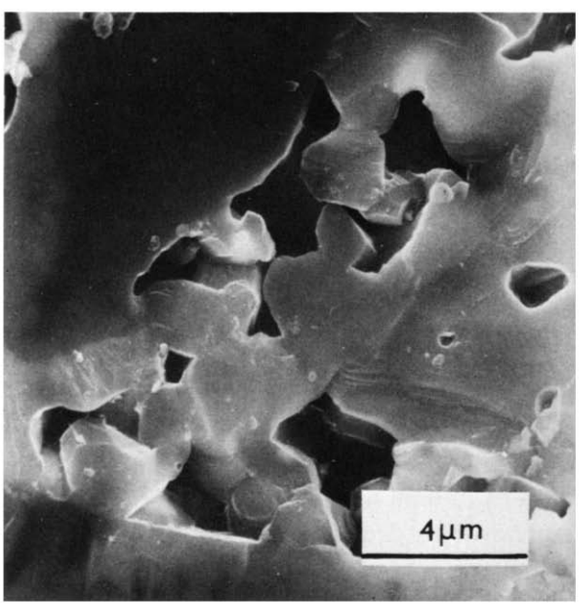

Fig. 5. SEM micrograph of fracture surface of sample I (SiC–B_4C) sintered according to schedule a (Fig. 1).

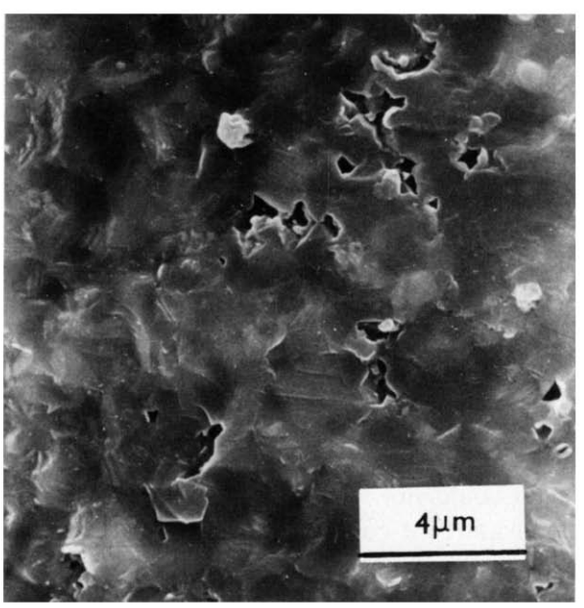

Fig. 6. SEM micrograph of fracture surface of sample II (Si–B–C) sintered according to schedule b (Fig. 1).

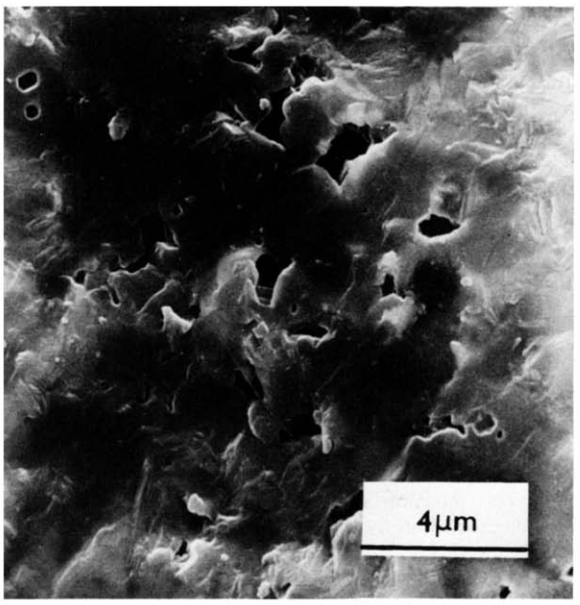

Fig. 7. SEM micrograph of fracture surface of sample IV (Si–B–C) sintered according to schedule c (Fig. 1).

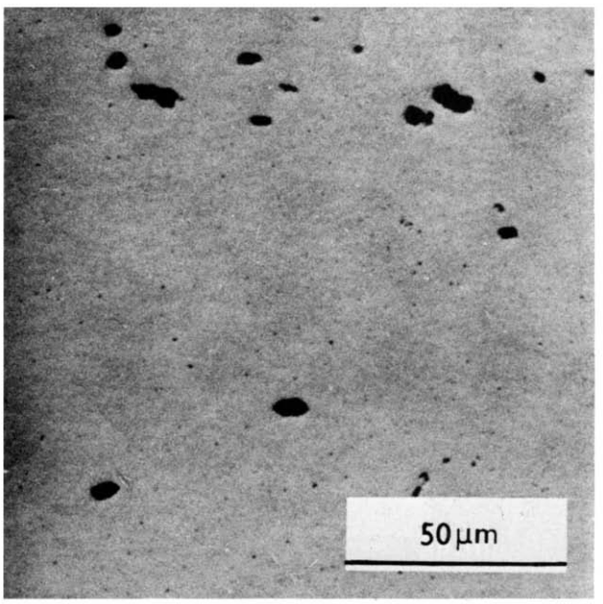

Fig. 9. Micrograph of polished surface of sample IV (Si–B–C) sintered according to schedule c (Fig. 1).

consolidation and maximum heating rate in the temperature range 1000–1800°C. Due to the discontinuous pressure new reaction contacts can be formed and therefore better conditions for the combustion and post-combustion densification were achieved. Immediately after combustion a considerable lowering of shrinkage rate was observed (Fig. 4(III–V)) as a consequence of extremely high temperature increase during combustion (high rate of thermal expansion) and a change from a non-diffusional densification to a diffusional one.

The lower final densities and relatively high FSR were determined after consolidation without pressure shocks (schedules e and f in Fig. 1; Table 1), despite the high contribution to densification during combustion and highest possible heating rate up to the isothermic period of consolidation. These results emphasize the importance of the pressure–temperature schedule.

Comparing the final densities and microstructures of samples labelled as IV and V in Table 1, the pressure schedule particularly seems to be very important for the consolidation process. The fracture surfaces and polished sections of samples IV and V are shown in Figs 7–10, and there are evident differences between the number and size of pores. A smaller number of small pores can be estimated for sample IV from Fig. 9, while no large pores were observed in sample V (Fig. 10). It is supposed that the partial elimination of small pores

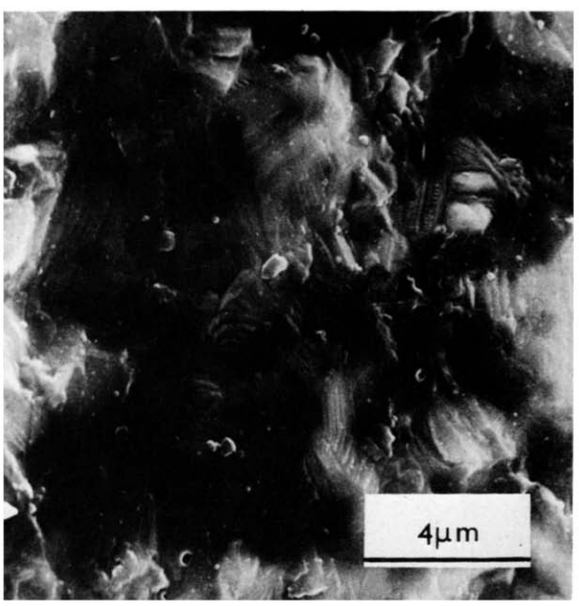

Fig. 8. SEM micrograph of fracture surface of sample V (Si–B–C) sintered according to schedule d_1 (Fig. 1).

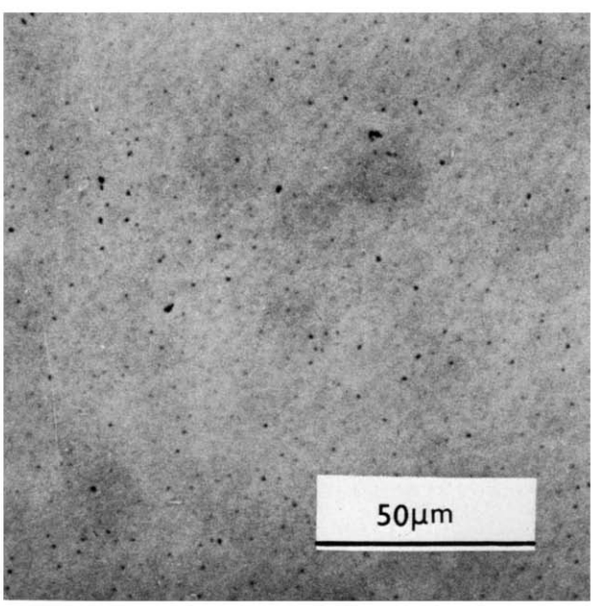

Fig. 10. Micrograph of polished surface of sample V (Si–B–C) sintered according to schedule d_1 (Fig. 1).

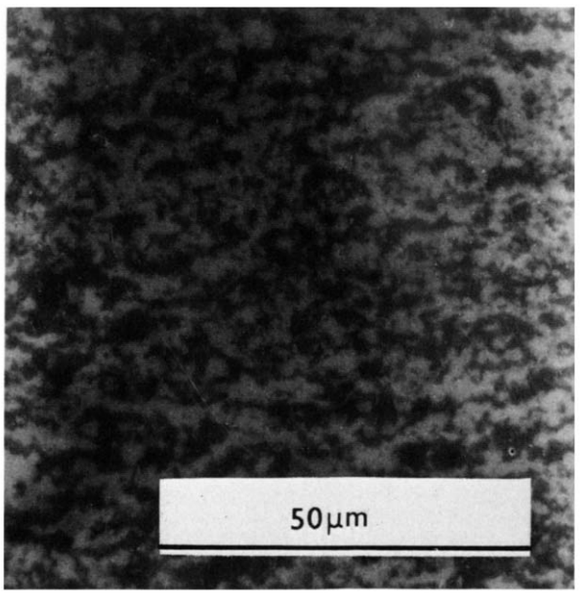

Fig. 11. SEM micrograph of polished surface of sample VI (Si–B–C) sintered according to schedule d_2 (Fig. 1).

in sample IV is due to the longer dwell at maximum temperature. The considerably lower porosity of sample V is probably due to the discontinuous pressure in the initial stage of consolidation, because the other parameters were identical.

The former explanation of elimination of small pores confirms the microstructure of sample VI (Fig. 11), which is characterized by the two solid phases (SiC and B_4C) in the form of interlocked matrices with very low porosity.

However, further experiments are needed to explain this behaviour and to optimize the pressure–temperature treatment schedule.

4 Conclusions

Powder mixtures of silicon, boron and carbon black can be converted into a ceramic material with a very low porosity and uniform microstructure by the method of combustion hot-pressing (CHP). The final density of material after CHP depends strongly on the temperature–pressure treatment schedule. Particularly, the pressure schedule before ignition seems to be very important.

References

1. Yajima, S., Special heat-resisting materials from organo-metallic polymers. *Ceram. Bull.*, **62** (1983) 893–915.
2. Wills, R. R., Markle, R. A. & Mukherjee, S. P., Siloxanes, silanes, and silazanes in the preparation of ceramics and glasses. *Ceram. Bull.*, **62** (1983) 904–15.
3. Hurwitz, F. I., Gyekenyesi, J. Z. & Conroy, P. J., Polymer derived Nicalon/Si–C–O composites: processing and mechanical behaviour. *Ceram. Eng. Sci. Proc.*, **10** (1989) 750–3.
4. Rees, W. S. Jr & Seyfert, D., Preparation, characterization and pyrolysis of decaborane (14)-based polymers: B_4C/BN and BN procedures. *Ceram. Eng. Sci. Proc.*, **10** (1989) 837–45.
5. Borovinskaja, I. P. & Merzhanov, A. G., Synthesis of high-temperature nonmetallic ceramics by combustion processes. In *Proceedings of 1st International Conference Interprogress '88*. Dom Techniky, Bratislava, 1988, pp. 10–13.
6. Meerson, G. A. & Samsonov, G. V., *Zavod. lab.*, **16** (1950) 1423–8.
7. Uhrik, M., Laboratory equipment for hot-pressing. *Ceramics-Silikáty*, **35** (1991) 147–53.
8. Barin, I. & Knacke, O., *Thermochemical Properties of Inorganic Substances*. Springer-Verlag, Berlin, 1973.
9. Jansson, B. & Agren, J., A thermochemical assessment of liquid–solid equilibria in nickel-rich Ni–Si–B alloys. *Mat. Sci. Eng.*, **63** (1984) 51–60.
10. Kuzenkova, M. A., Kislyj, P. S., Grabchuk, B. L. & Bondaruk, N. I., The structure and properties of sintered boron carbide. *J. Less-Common Met.*, **67** (1979) 217–23.
11. Kislyj, P. S., Kuzenkova, M. A., Bondaruk, N. I. & Grabchuk, B. L., *Karbid bora (Boron Carbide)*. Naukova Dumka, Kiew, 1988, pp. 107–50.
12. Dole, S. L. & Prochazka, S., Densification and microstructure in boron carbide. *Ceram. Eng. Sci. Proc.*, **6** (1985) 1151–60.
13. Kislyj, P. S. & Samsonov, G. V., Diffuzija bora v uglerode (The diffusion of boron in carbon). *Fizika tvjordovo tela*, **2** (1960) 1729–32.